Cerium(III) and cerium(IV) nitrate complexes of trialkylphosphine oxides

Coles Simon J[1], Sarah J. Fieldhouse[2], Wim T. Klooster[1] and Andrew W. G. Platt[2]*

1. UK National Crystallography Service, Chemistry, University of Southampton, Highfield Campus, Southampton, SO17 1BJ, UK

2. School of Law Policing and Forensic Science, Staffordshire University, Leek Road, Stoke-on-Trent, ST4 2DF, UK

Abstract

The reactions of ammonium cerium(IV) nitrate, $(NH_4)_2Ce(NO_3)_6$ (CAN) with trialkylphosphine oxides, R_3PO (R= Et, ^iPropyl, $^nBu_3$, $^iBu_3PO$, $^tBu_3PO$, Cy_3PO (Cy = cyclohexyl) and Oct_3PO (Oct = n-octyl)) have been investigated by 31-P NMR spectroscopy in a variety of conditions. Reactions with acetone solutions of excess of CAN and R_3PO and of solid CAN with chloroform solutions of R_3PO and aqueous solutions of CAN with chloroform solutions of R_3PO led to the observation of $Ce(NO_3)_4(R_3PO)_2$. 31-P NMR spectroscopy and conductimetric titration of acetone solutions of CAN with R_3PO confirm the initial reactions is the formation of $Ce(NO_3)_4(R_3PO)_2$ (R = Et, Bu, Cy, Oct) followed by a slower reaction to form the ionic $[Ce(NO_3)_3(R_3PO)_3][NO_3]$. The isolation of pure cop-lexes has not proved possible in most cases but crystals suitable for x-ray analysis were extracted in some instances. The structures of the Ce(IV) complexes $[Ce(NO_3)_4(Cy_3PO)_2]$ and $[Ce(NO_3)_3(Et_3PO)_3][NO_3]$ and the related Ce(III) complexes $[Ce(NO_3)_3(Cy_3PO)_3]$ and $[Ce(NO_3)_3(H_2O)_3(Et_3PO)]$ are reported.

Introduction

Whilst many cerium(IV) complexes are known with a variety of ligands [1] complexes with phosphine oxides are rather rare[1,2]. Given the large number of coordination compounds between trivalent lanthanides (including cerium(III)) and phosphine oxides [2] this is surprising. The synthesis and structure of $Ce(NO_3)_4(Ph_3PO)_2$ by reaction of ceric ammonium nitrate (CAN) with triphenylphosphine oxide in acetone was reported in 1971 [3] but since then no structures of Ce(IV) nitrate with phosphine oxides have been reported. A thermally unstable complex with $Ph_2P(O)CH_2C(O)Ph$ was isolated and characterised as $Ce(NO_3)_3(Ph_2P(O)CHC(O)Ph)(Ph_2P(O)CH_2C(O)Ph)_2$ on the basis of elemental analysis and infrared spectroscopy[4]. A cerium(IV) complex, $Ce(NO_3)_4(^tBuPhPOC_2H_4POPh^tBu)$ was prepared from CAN and the

ligand in acetone and characterised by spectroscopy and elemental analysis but the structure was not reported [5]. The complex $Ce(NO_3)_3((n-C_8H_{17})PhP(O)CH_2N^iBu_2)_3$ undergoes reversible one electron oxidation in acetonitrile solution but the Ce(IV) complex formed was not further characterised [6]. In view of the relative lack of studies on Ce(IV) nitrate - phosphine oxide complexes we report our study of the reactions between CAN and a variety of trialkyl phosphine oxides. In particular we hoped to establish whether the synthesis was applicable to other R_3PO and if the previously reported structure for $Ce(NO_3)_4(Ph_3PO)_2$ is typical of Ce(IV) nitrate - phosphine oxide complexes.

Results and discussion

We report three types of reaction which have been carried out in an attempted to prepare Ce(IV) complexes. All the reactions use CAN as the source of Ce(IV) and differ only in the solubility of various components in the solvent systems employed. The overall reaction is indicated below

$$(NH_4)_2Ce(NO_3)_6 \quad + \quad 2R_3PO \quad \rightarrow \quad Ce(NO_3)_4(R_3PO)_2 \quad + \quad 2 NH_4NO_3$$
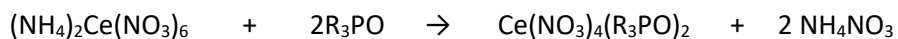
A solvent in which both CAN, R_3PO and the Ce(IV) phosphine oxide complex are soluble, and in which ammonium nitrate is not was chosen. Acetone has been previously employed for this type of reaction and we have found this and acetonitrile to be appropriate solvents.

The reaction using an aqueous / chloroform biphasic solvent system in which CAN and ammonium nitrate remain in the aqueous phase and the phosphine oxide and the Ce(IV) complexes remain in the organic layer offers a potentially attractive synthesis allowing for easy separation of the product.

Reactions between a chloroform solution of R_3PO and solid CAN is also attractive as the Ce(IV) complex would be the only chloroform soluble product.
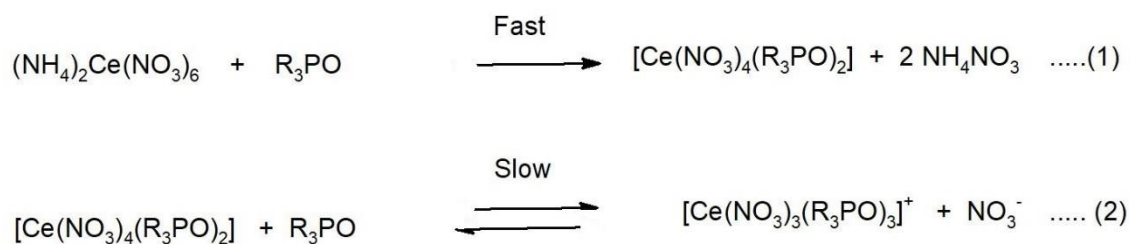

Solution NMR and conductivity study

Reactions between CAN and R_3PO were studied in deuterated acetone and chloroform.

In acetone the reactions in 1:1 and 1:2 CAN: R_3PO, (R=Et, iPr, Bu, Oct), ratios gave a single sharp signal assigned to $Ce(NO_3)_4(R_3PO)_2$. With higher ratios of R_3PO the sharp peak was initially superimposed on a

broad signal ($W_{1/2}$ about 400 – 500 Hz) and on standing the spectra showed only a broad signal. These

observations are consistent with the formation of 1:3 complexes, possibly $[Ce(NO_3)_3(R_3PO)_3]^+NO_3^-$ (see

below) in dynamic equilibrium with free R_3PO as indicated in Scheme 1.

<div align="center">

Scheme 1

The reaction between R_3PO and CAN

</div>

$$(NH_4)_2Ce(NO_3)_6 \quad + \quad R_3PO \quad \xrightarrow{\text{Fast}} \quad [Ce(NO_3)_4(R_3PO)_2] \; + \; 2\,NH_4NO_3 \quad .....(1)$$

$$[Ce(NO_3)_4(R_3PO)_2] \; + \; R_3PO \quad \underset{\longleftarrow}{\overset{\text{Slow}}{\rightleftharpoons}} \quad [Ce(NO_3)_3(R_3PO)_3]^+ \; + \; NO_3^- \quad ..... (2)$$

Variable temperature 31-P NMR studies were carried out between -40 to 50°C with a range of R (R= Et, Bu

and Oct) to confirm this. At -40°C the spectra for the CAN/Et_3PO system are resolved into two broad ($W_{1/2}$

about 500 Hz) peaks at 110.0 and 71.2 ppm, which on warming to -20°C coalesce into a single broad peak

($W_{1/2}$ 1 kHz) which becomes sharper with increasing temperature indicative of increasingly rapid exchange

giving a resonance at 87.8 ppm ($W_{1/2}$ 270 Hz) at 50°C. The spectra for R= Bu and Oct were similar with the

exception that the separate signals for the Oct_3PO / CAN system were not resolved at low temperature

implying faster exchange than observed for the smaller phosphine oxides. A typical set of spectra is shown

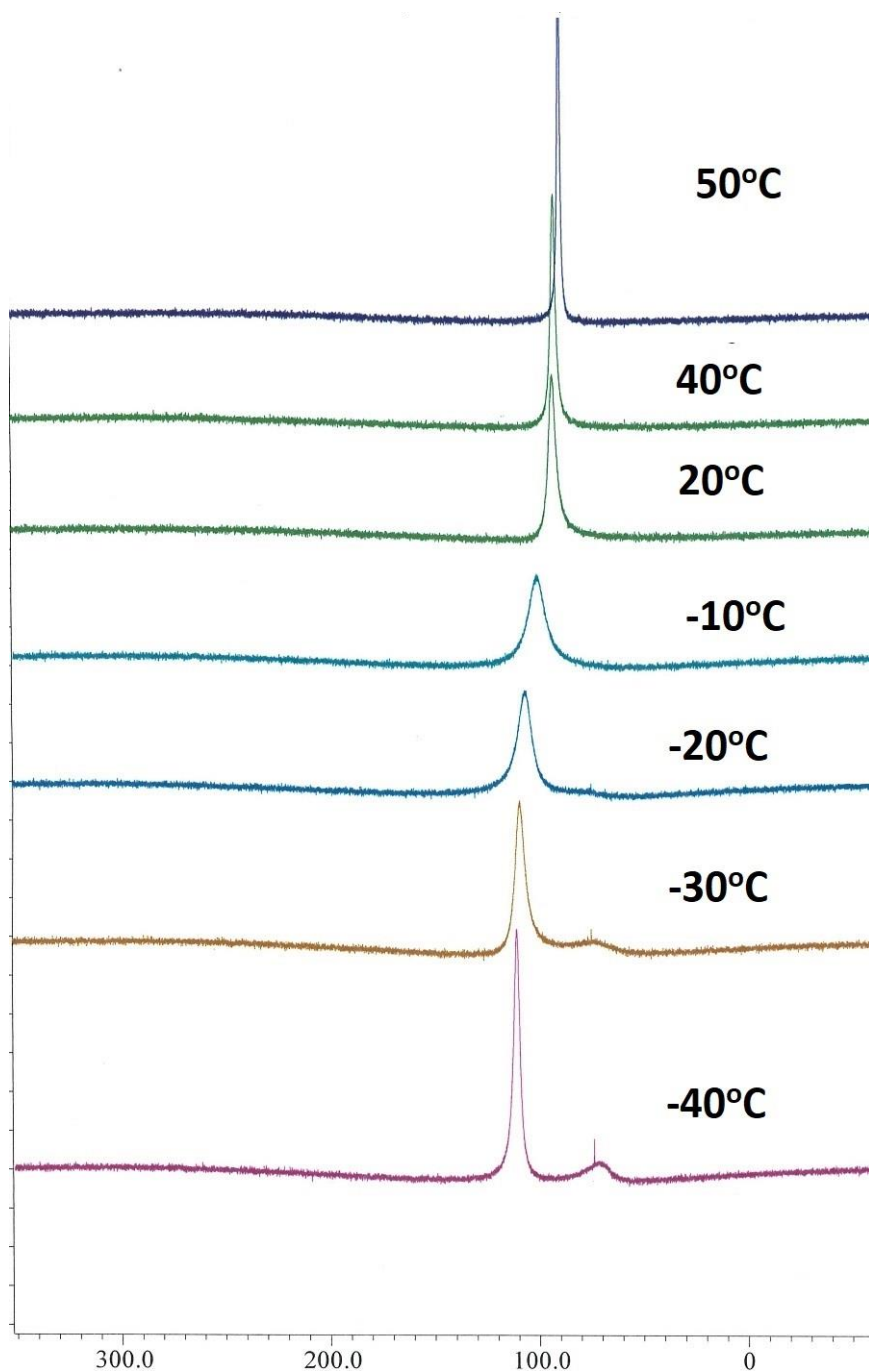for the CAN / Et_3PO system in Figure 1

Figure 1 The variable temperature 31-P NMR spectra of the CAN / Et$_3$PO system in d$_6$ acetone

Further confirmation was obtained from conductivity titrations in acetone and a typical plot is shown in Figure 1. The conductivity of a solution of CAN decreased on addition of R$_3$PO until a 2:1 ratio and remained constant thereafter, consistent with the formation of insoluble ammonium nitrate and neutral Ce(NO$_3$)$_4$(R$_3$PO)$_2$ complex (equation (1)). The conductivities of the 3:1 solution slowly increase on standing, consistent with displacement of nitrate ion from the coordination sphere of the metal (equation (2)).
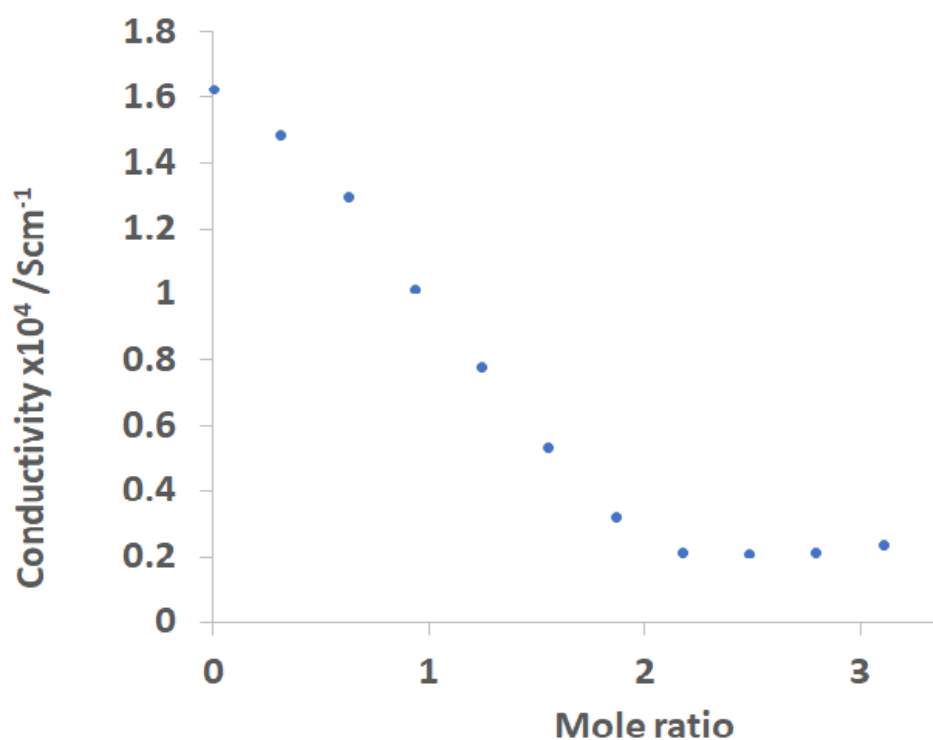
Figure 2 Conductivity 0.02 M CAN vs Bu₃PO in acetone

The reaction of solutions of R_3PO in $CDCl_3$ with an excess (CAN:R_3PO >4:1) of solid CAN become yellow / orange in colour soon after mixing. The 31-P NMR spectra clearly indicate the formation of Ce(IV) complexes giving sharper lines at significantly different chemical shifts to the either the analogous Ce(III) complexes or the unreacted R_3PO. The 31-P NMR data are shown in Table 1 and the 13-C data are given in Table S1. In the initial stages of the reaction when R_3PO was in excess two separate signals were seen in the 31-P spectra due to the Ce(IV) complex and unreacted ligand showing that exchange between the two is not rapid on the NMR timescale at 20°C.

Biphasic reactions between aqueous solutions of CAN and chloroform solutions of R_3PO proceed rapidly on mixing giving spectra identical to those obtained from the R_3PO / solid CAN systems. The exchange reaction between chloroform solutions of $Ln(NO_3)_3(R_3PO)_3$ and either solid or aqueous solutions of CAN gives Ce(IV) phosphine oxide complexes with identical chemical shifts to those found using the other methods described above. In this case there is no rapid exchange between $Ln(NO_3)_3(R_3PO)_3$ which generally have very large line widths and the Ce(IV) complexes.

R	Ce(NO$_3$)$_4$(R$_3$PO)$_2$	Ce(NO$_3$)$_3$(R$_3$PO)$_3$	R$_3$PO
Et	79.9	100.8[a]	53.2
iPr	86.7	109.7[b]	60.8
nBu	75.4		49.2
iBu	76.0	91.2[c]	46.9
tBu	74.0	94.8[d]	66.6
Cy	78.5	101.5	51.7
Oct	75.1		49.1

Table 1

31-P NMR data for the cerium(III) and cerium(IV) complexes in CDCl$_3$

a. Data from ref 7, b. data from ref 8, c. data from ref 9, d. data from ref 10

Attempts to prepare ionic complexes with other counterions were made by reaction of CAN/ R$_3$PO/ KPF$_6$, CAN / R$_3$PO / NaBPh$_4$ were not successful.

Solid State study

The complex Ce(NO$_3$)$_4$(Cy$_3$PO)$_2$ was prepared by the biphasic reaction of aqueous CAN and chloroform solution of Cy$_3$PO and isolated by cooling a chloroform / diethyl ether mixture giving the product as yellow needles which were suitable for x-ray crystal structure determination.

Details of the data collection and refinement are given as supplementary information and selected bond lengths and angles in Table S2.   ORTEP plots showing the thermal motion at 50% probability level are also given in the supplementary information. Two views of the structure are shown in Figure 3.

The overall geometry is similar to that reported for the Ph$_3$PO complex [3] with an equatorial belt of bidentate nitrates and axial phosphine oxides giving a coordination number of 10.   Analysis of the geometry of the coordination polyhedron was carried out by continuous shape measures [11] using the SHAPE programme [12]. This gives an objective measure of the deviation of the structure from idealised polyhedral for the given coordination number, and in this case gives a bicapped square antiprism as the

best description of the structure with the square planes defined by O1, O3, O6 and O7 with O4 capping.

The two planes are almost parallel with an angle between them of 1.5°.
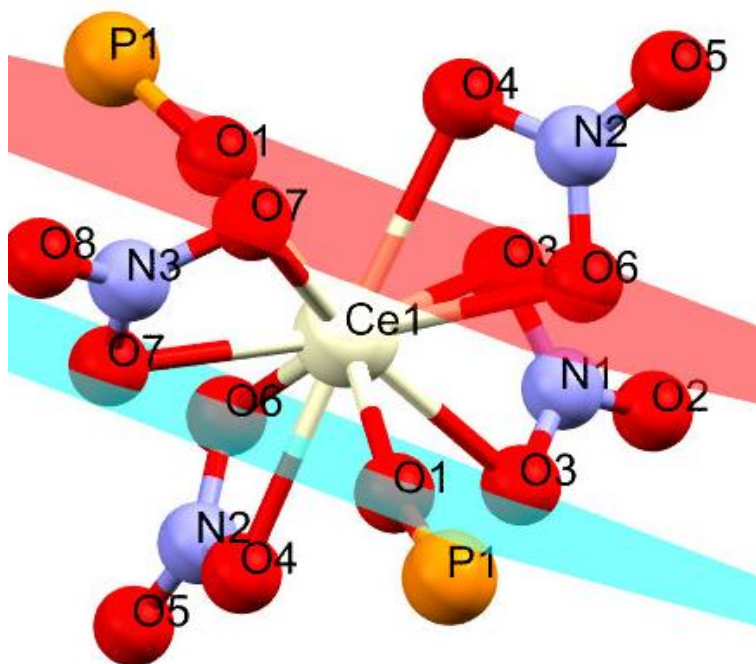
A
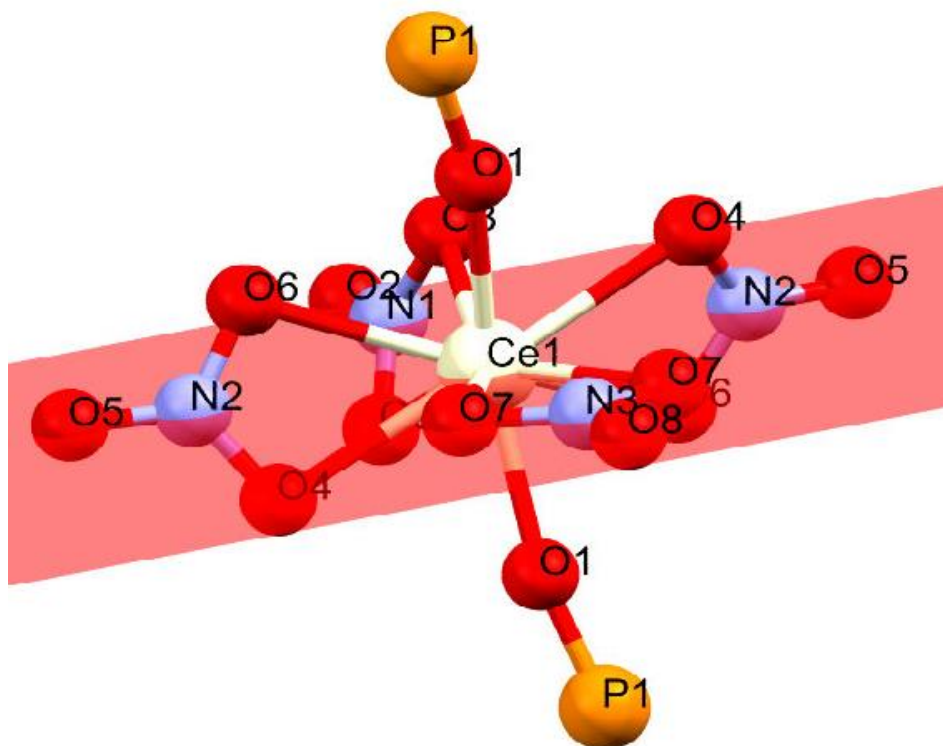
B

Figure 3 Two views of the structure of Ce(NO$_3$)$_4$(Cy$_3$PO)$_2$ (cyclohexyl groups omitted for clarity) A showing the bicapped square antiprismatic geometry and B a pseudo octahedral geometry

The complex is rather more symmetrical than Ce(NO$_3$)$_4$(Ph$_3$PO)$_2$ in that the 4 N-atoms, the cerium ion and the terminal oxygen atoms of all nitrates are all coplanar as indicted in Figure 2B. One of the nitrate groups lies entirely in the CeN4 plane whilst the others are twisted with an angle of about 70° between the CeN4 and NO3 planes. The average Ce-O(P) distance at 2.239 Å is slightly longer than 2.219 Å for the Ph$_3$PO complex, probably due to the increased steric hindrance of the cyclohexyl groups which balances the probable increase in negative charge at the oxygen of Cy$_3$PO compared to Ph$_3$PO. The distances to the nitrate oxygen atoms are essentially the same. The corresponding distances in the Ce(III) complexes show the trend expected with Ce-O(P) distances shorter in the Cy$_3$PO complex with the Ce-O(N) distances being the same as for the Ph$_3$PO complex. Compared to the Ce(III) derivative the Ce-O distances are all shorter as expected from the smaller ionic radius of Ce(IV) compared to Ce(III).

Table 2				
Comparison of selected average bond distances (Å) and angles in Ce(IV) and Ce(III) complexes[a]				
	Ce(NO$_3$)$_4$(Ph$_3$PO)$_2$[b]	Ce(NO$_3$)$_4$(Cy$_3$PO)$_2$[c]	Ce(NO$_3$)$_3$(Ph$_3$PO)$_3$[d]	Ce(NO$_3$)$_3$(Cy$_3$PO)$_3$[c]
Ce-O(P)	2.219(4)	2.239(0)	2.414(11)	2.391(1)
Ce-O(N)	2.478(27)	2.482(14)	2.608(26)	2.597(17)
P-O	1.528(3)	1.528(0)	1.487(15)	1.512(7)
(P)O-Ce-O(P)	155.0	157.8		
Cerium Ionic radii[e]	1.07	1.07	1.196	1.196

a. Values in parenthesis are standard deviations which reflect the variation in bond distances rather than uncertainties in the data collection. b. Data from ref 3, c. this work, d. data from ref 13. e. 10-coordinate radius for Ce(IV) and 9-coordinate radius for Ce(III)

The infrared spectra of the Ce(IV) complex show the expected bands due to coordinated nitrate in similar positions to those observed in $Ce(NO_3)_3(Cy_3PO)_3$. The splitting of ν_3 is increased from 31 to 69 cm^{-1} which are seen as intense bands at 1446 and 1514 cm^{-1}. The PO stretch is at considerably reduced wavenumber in the Ce(IV) complex, 1019 cm^{-1} compared to 1095 cm^{-1} in $Ce(NO_3)_3(Cy_3PO)_3$ consistent with the longer P-O bond (the P-O stretch in the free ligand is at 1146 cm^{-1}).

Attempts to isolate complexes with less sterically demanding phosphine oxides by this biphasic reaction method were not successful. Reaction aqueous solution of CAN with chloroform solution of Et_3PO led to the formation of $Ce(NO_3)_4(Et_3PO)_2$ in the organic layer (31-P NMR evidence). Separation of the layers followed dry drying ($MgSO_4$) and evaporation led to an oil which could not be crystallised by normal methods. On prolonged standing this oil partially solidified and crystals suitable for x-ray diffraction studies could be extracted from it. The crystals were the Ce(III) complex $Ce(NO_3)_3(H_2O)_3(Et_3PO)$ the structure of which is shown in Figure 4. The coordinated water molecules arise as a result of the preparative method. The complex can be considered as a distorted pentagonal bipyramid if the nitrate ligands are thought of as pseudo monodentate ligands bonded through the nitrogen atom.
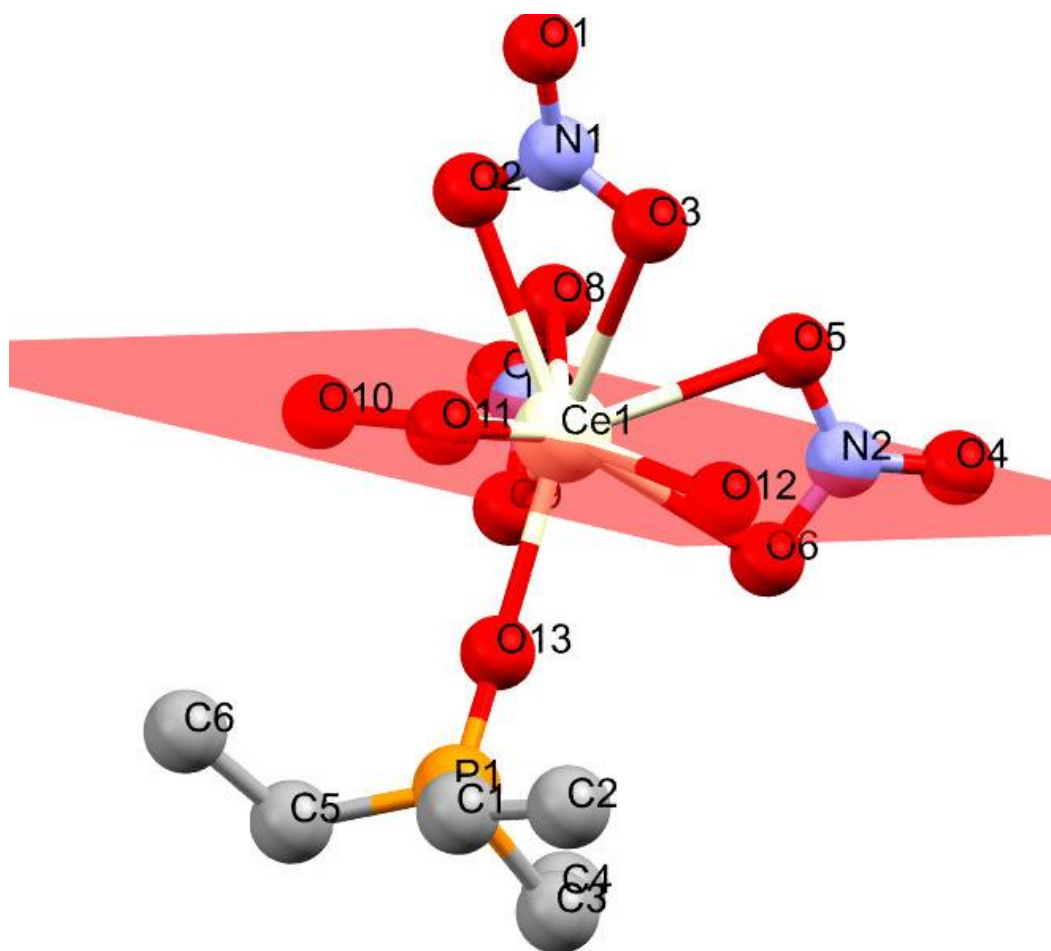
Figure 4 The structure of Ce(NO₃)₃(H₂O)₃(Et₃PO) (hydrogen atoms omitted for clarity)

The equatorial plane is defined by the two remaining nitrate nitrogen atoms and the three water oxygen atoms. The bond distances compare well with those observed in the structure of $Ce(NO_3)_3(Et_3PO)_3$ and are shown in Table 3. All the bond distances agree well with those observed in $Ce(NO_3)_3(Et_3PO)_3$.

Reaction of chloroform solutions of R_3PO with solid CAN gave $[Ce(NO_3)_4(R_3PO)_2]$ as the only phosphorus containing species in solution. Evaporation of these solutions produced viscous intractable oils for which only modest to poor elemental analysis could be obtained. The triethylphosphine oxide complex was studied in more detail. Exhaustive attempts to produce crystalline solids using a variety of techniques failed. On prolonged standing the oil gave a small amount of crystalline material which could be mechanically extracted from the viscous oil and were suitable for x-ray diffraction. These crystals were the ionic complex $[Ce(NO_3)_3(Et_3PO)_3]^+ [NO_3]^-$, the cation of which has a pseudo-octahedral geometry taking the nitrates as monodentate ligands attached via the nitrogen atoms. The structure is shown in Figure 5. There are voids (channels) in the structure of about 360 Å^3 and the ionic nitrate was not refined. However,

the infrared spectrum clearly indicates the presence of ionic as well as coordinated nitrates. Intense absorptions at 1507, 1432, 1317 and 1263 cm^{-1} are assigned to coordinated bidentate nitrates and a medium intensity peak at 1403 cm^{-1} to ionic nitrate. The large splitting in ν_3 is again observed and together with the large overall splitting of the nitrate absorptions seems to be a characteristic feature of the spectra of Ce(IV) nitrate complexes.

Analysis by continual shape measures gives a tricapped trigonal prism as the best description of the geometry around the Ce ion. The triangular faces, formed by the O1 oxygen atoms and the O4 atoms from the phosphine oxides, are parallel. The capping atoms are O2 from the nitrates and the angles between the square faces at 60.04° correspond closely to the idealised angles of 60°.
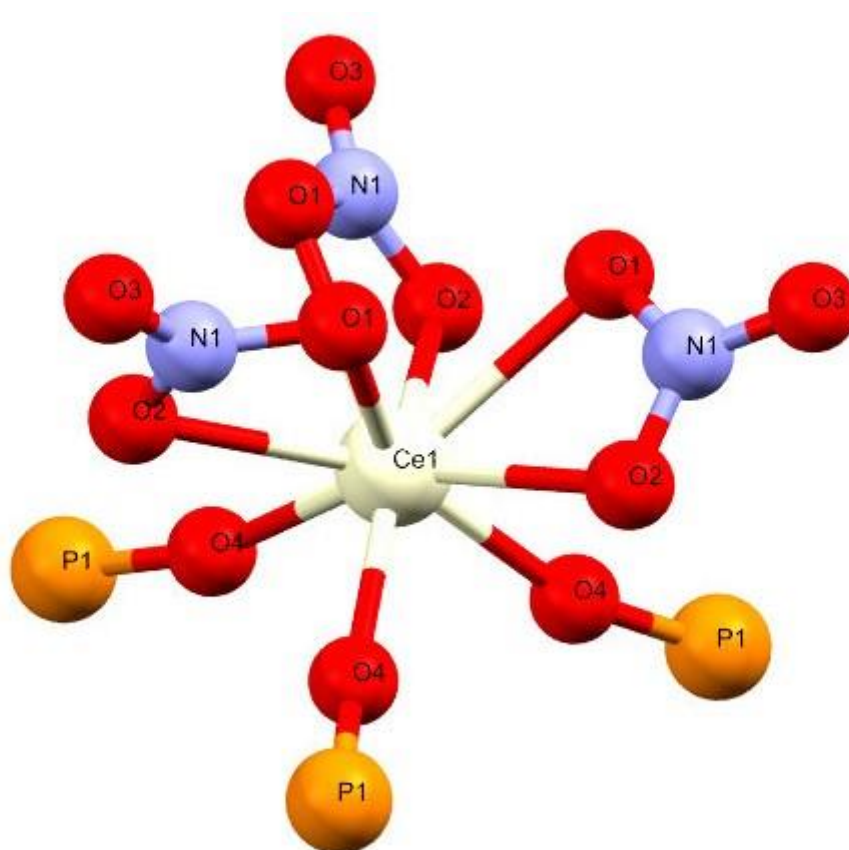
Figure 5 The structure of the [*fac*-Ce(NO₃)₃(Et₃PO)₃]⁺ cation (ethyl groups omitted for clarity)

Selected bond distances are compared with those of *mer*- Ce(NO₃)₃(Et₃PO)₃ [8] and Ce(NO₃)₃(H₂O)₃(Et₃PO) in Table 3. All the bonds to Ce in [*fac*-Ce(NO₃)₃(Et₃PO)₃]⁺ are significantly shorter than in *mer*-Ce(NO₃)₃(Et₃PO)₃ which implies the compound is actually Ce(IV) rather than Ce(III).

<div align="center">

Table 3

Comparison of selected average bond distances in Ce(III) and Ce(IV) Et₃PO complexes with

calculated oxidation states

</div>

	$[fac\text{-}Ce(NO_3)_3(Et_3PO)_3]^+$	$mer\text{-}Ce(NO_3)_3(Et_3PO)_3{}^b$	$Ce(NO_3)_3(H_2O)_3(Et_3PO)$
Ce-O(P)	2.199(1)^a	2.374(17)	2.317
Ce-O(N)	2.483(26)	2.605(21)	2.651(26)
P-O	1.530(0)	1.499(7)	1.504
BVS +3^c	4.66	3.12	3.03
BVS +4^c	4.09	2.74	2.67

a. Values in parenthesis are standard deviations which reflect the variation in bond distances rather than the data collection. b. data from ref 7 c. from ref 12 $BVS + 3 = \sum_i e^{(2.188 - ri)/0.37}$ $BVS + 4 = \sum_i e^{(2.07 - ri)/0.37}$

Bond valence sums (BVS) [14] provide a method of estimating the oxidation state in cases where there is ambiguity from the structural data such as here where the anion is disordered or where the hydrogen atoms of coordinated water molecules or hydroxide may be difficult to detect. The calculated bond valence sums for both +3 and +4 oxidation states are given in Table 3. The values of BVS were calculated on the basis of the oxidation state being either +3 or +4 and both results are presented in the table. The sum should closely match the true oxidation state and clearly show that the $[Ce(NO_3)_3(Et_3PO)_3]^+$ is correctly formulated as Ce(IV) and $Ce(NO_3)_3(H_2O)_3(Et_3PO)$ as Ce(III).

Conclusion

Cerium(IV) complexes of trialkylphosphine oxides can be readily formed in solution although isolation has proved to be difficult for all but the tricyclohexylphosphine oxide complex. Analysis of structures using bond valence sums has provided a means of assigning oxidation states in cases where the structural data is ambiguous and shown that cationic cerium(IV) species can be formed. The geometries around the cerium ion were found to be best described as a bicapped square antiprism for $Ce(NO_3)_4(Cy_3PO)_2$ and a tricapped trigonal prism for $[Ce(NO_3)_3(Et_3po)_3]^+$. Attempts to isolate cationic complexes as the PF_6^- or BPh_4^- salts was not successful.

Experimental

NMR spectra were recorded in $CDCl_3$ solution on a JEOL ECX 400, approximately 20 mg of solid in 1 mL of the appropriate deuterated solvent.

Infrared spectra were recorded with a resolution of ± 1 cm^{-1} on a Thermo Nicolet Avatar 370 FT-IR spectrometer operating in ATR mode. The samples were compressed onto the optical window and spectra recorded without further sample pre-treatment.

X-Ray crystallography

Full details of the data collection and refinement are given as supplementary information. Crystallographic data (excluding structure factors) for the structures in this paper have been deposited with the Cambridge Crystallographic Data Centre as supplementary publication numbers 1879338, 1879342, 187943 and 1879350 for $Ce(NO_3)_4(Cy_3PO)_2$, $Ce(NO_3)_3(H_2O)_3(Et_3PO)$, $[Ce(NO_3)_3(Et_3PO)_3][NO_3]$ and $Ce(NO_3)_3(Cy_3PO)_3$ respectively. Copies of the data can be obtained, free of charge, on application to CCDC, 12 Union Road, Cambridge CB2 1EZ, UK (Fax: þ44(0)-1223-336033 or e-mail: deposit@ccdc.cam.ac.uk

Synthesis

$Ce(NO_3)_4(Cy_3PO)_2$ An excess of CAN (0.45 g 0.82 mmol) in 2.5 mL water were stirred with a solution of Cy_3PO (0.24 g 0.81 mmol) in 1.8 mL of chloroform for 10 minutes. The orange chloroform layer was

separated, dried (MgSO$_4$), filtered and mixed with an equal volume of diethylether. Cooling to -30°C gave yellow needles suitable for x-ray crystallography (0.19 g 46% based on Cy$_3$PO**).** Analysis (%) Expected (found): C 44.08 (44.92) H6.78 (6.73) N 5.71 (5.69)

Ce(NO$_3$)$_4$(Et$_3$PO)$_2$; CAN (92.0 mg 0.17 mmol) was suspended with Et$_3$PO (29.8 mg 0.22 mmol) in 0.6 mL CDCl$_3$. After the 31-P NMR spectrum indicated complete reaction the solution was filtered evaporated to dryness and the resulting yellow oil dried in vacuo over KOH to give 38.6 mg (53 %).

On standing the oil partially solidified and crystals of [Ce(NO$_3$)$_3$(Et$_3$PO)$_3$][NO$_3$] suitable for x-ray diffraction studies were mechanically removed. There was insufficient material for elemental analysis.

NMR (CDCl$_3$) 31-P δ 79.9 ppm 13-C CH$_3$ δ 4.95,δ(δ, ^{2}J$_{PC}$ = 4.7 Hz), CH$_2$ 18.35 9d, ^{1}J$_{PC}$ = 65.1 Hz)

Analysis (%) Expected (found): C 22.96 (23.44) H 4.61 (4.89) N 8.54 (7.65)

Ce(NO$_3$)$_4$(Bu$_3$PO)$_2$; CAN (69.8 mg 0.13 mmol) was suspended with Bu$_3$PO (34.4 mg 0.16 mmol) in 0.6 mL CDCl$_3$. After 6 d the 31-P NMR spectrum indicated complete reaction. The solution was filtered evaporated to dryness and the resulting yellow oil dried in vacuo over KOH to give 44.1 mg (67 %).

NMR (CDCl$_3$) 31-P δ 75.4 ppm 13-C CH$_3$ δ 13.46(s), CH$_2$ δ 22.95(d, ^{2}J$_{PC}$ = 3.8 Hz), CH$_2$ δ 24.03(d, ^{3}J$_{PC}$ =15.4 Hz), CH$_2$ δ 25.79(d, ^{1}J$_{PC}$ = 63.0 Hz)

Analysis (%) Expected (found): C 34.95 (38.18) H 6.60 (6.71) N 6.79 (7.65)

Ce(NO$_3$)$_4$(Oct$_3$PO)$_2$; CAN (68.0 mg 0.12 mmol) was suspended with Oct$_3$PO (50.0 mg 0.13 mmol) in 0.6 mL CDCl$_3$. After the 31-P NMR spectrum indicated complete reaction. The solution was filtered, evaporated to dryness and the resulting yellow oil dried in vacuo over KOH to give 45.0 mg (60 %).

NMR (CDCl$_3$) 31-P δ 75.1 ppm 13-C δ 14.16(s), δ 21.01 (d, ^{2}J$_{PC}$ = 3.8 Hz), δ 23.20 (d, ^{1}J$_{PC}$ = 63.2 Hz), δ 28.92(s), δ 29.03(s), δ 30.90 (d, ^{3}J$_{PC}$ = 15.3 Hz), δ 31.81(s)

Analysis (%) Expected (found): C 49.64 (53.62) H 8.85 (9.38) N 4.82 (4.57)

References

1. Y-M. So, W-H. Leung, Coord. Chem. Rev. **340** (2017) 172

2. A.W.G. Platt, Coord. Chem. Rev. **340** (2017) 21

3. M. Ul-Haque, C.N. Caughlin, F.A. Hart, R. vanNice, Inorg. Chem. 10 (1971) 115

4. R. Babecki, A.W.G. Platt and R.R. Russell, Inorg. Chim. Acta 171 (1990) 25

5. Y. Koide, A. Sakamoto, T. Imamoto, T. Tanase, Y. Yamamoto, J. Alloys Compnd. 192 (1993) 211

6. P-Y Jiang, Y. Ikeda, M. Kumagai J. Nucl. Sci. Tech. 31 (1994) 491

7. A. Bowden, K. Singh, A.W.G. Platt, Polyhedron 42 (2012) 30

8. A. Bowden, S.J. Coles, M.B. Pitak, A.W.G.Platt, Polyhedron 68 (2014) 258

9. A. Bowden, P.N. Horton, A.W.G. Platt, Inorg. Chem. 50 (2011) 2553

10. A. Bowden, S.J. Coles, M.B. Pitak, A.W.G.Platt, Inorg. Chem. 51 (2012) 4379

11. S.Alvarez, P.Alemany, D.Casanova, J.Cirera, M.Llunell, D.Avnir, Coord. Chem. Rev. **249**, (2005), 1693

12. M.Llunell, D.Casanova, J.Cirera, P.Alemany, S.Alvarez, SHAPE – Program for the Stereochemical Analysis of Molecular Fragments by Means of Continuous Shape Measures and Associated Tools, Version 2.1, University of Barcelona, Spain, 2013Shape

13. W. Levason, E.H. Newman, M. Webster, Polyhedron 19 (2000) 2697

14. G.J. Palenik, S-Z. Hu, Inorg. Chim. Acta 362 (2009) 4740

15. S.J.Coles, P.A.Gale, Chem. Sci., 3 (2012) 68

Crystal Data and Experimental for Ce(NO$_3$)$_4$(Cy$_3$PO)$_2$
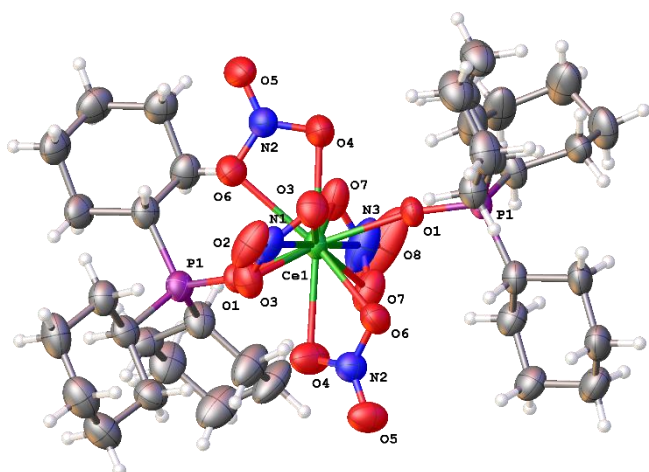
Experimental. Single yellow needle-shaped crystals of (**2017ncs0302**) were recrystallised from a mixture of chloroform and diethylether by solvent layering. A suitable crystal (0.300×0.050×0.040) mm^3 was selected and mounted on a MITIGEN holder in perfluoroether oil on a Rigaku 007HF diffractometer equipped with Varimax confocal mirrors and an AFC11 goniometer and HyPix 6000 detector. The crystal was kept at T = 100(2) K during data collection. Using **Olex2** (Dolomanov et al., 2009), the structure was solved with the **ShelXT** (Sheldrick, 2015) structure solution program, using the Intrinsic Phasing solution method. The model was refined with version 2014/7 of **ShelXL** (Sheldrick, 2015) using Least Squares minimisation.

Crystal Data. C$_{36}$H$_{66}$N$_4$O$_{14}$P$_2$Ce, M_r = 980.98, monoclinic, C2/c (No. 15), a = 14.8612(4) Å, b = 16.7067(4) Å, c = 18.9890(5) Å, β = 109.044(3)°, α = γ = 90°, V = 4456.6(2) Å^3, T = 100(2) K, Z = 4, Z' = 0.5, μ(CuK$_\alpha$) = 9.127, 21330 reflections measured, 4197 unique (R_{int} = 0.0545) which were used in all calculations. The final wR_2 was 0.1145 (all data) and R_1 was 0.0409 (I > 2(I)).

Compound	2017ncs0302
Formula	C$_{36}$H$_{66}$N$_4$O$_{14}$P$_2$Ce
$D_{calc.}$/ g cm^{-3}	1.462
μ/mm^{-1}	9.127
Formula Weight	980.98
Colour	yellow
Shape	needle
Size/mm^3	0.300×0.050×0.040
T/K	100(2)
Crystal System	monoclinic
Space Group	C2/c
a/Å	14.8612(4)
b/Å	16.7067(4)
c/Å	18.9890(5)
α/°	90
β/°	109.044(3)
γ/°	90
V/Å^3	4456.6(2)
Z	4
Z'	0.5
Wavelength/Å	1.54184
Radiation type	CuK$_\alpha$
Θ_{min}/°	4.112
Θ_{max}/°	70.055
Measured Refl.	21330
Independent Refl.	4197
Reflections Used	4010
R_{int}	0.0545
Parameters	260
Restraints	0
Largest Peak	1.012
Deepest Hole	-0.970
GooF	1.134
wR_2 (all data)	0.1145
wR_2	0.1136
R_1 (all data)	0.0420
R_1	0.0409

Structure Quality Indicators

Reflections:

d min (Cu)	I/σ	Rint	complete at 2θ=140°
0.82	26.8	5.45%	99%

Refinement:

Shift	Max Peak	Min Peak	GooF
-0.002	1.0	-1.0	1.134

A yellow needle-shaped crystal with dimensions 0.300×0.050×0.040 mm^3 was mounted on a MITIGEN holder in perfluoroether oil. X-ray diffraction data were collected using a Rigaku 007HF diffractometer equipped with Varimax confocal mirrors and an AFC11 goniometer and HyPix 6000 detector, and equipped with an Oxford Cryosystems low-temperature device, operating at T = 100(2) K.

Data were measured using profile data from ω-scans of 0.5 ° per frame for 1.0 s using CuK$_\alpha$ radiation (Rotating anode, 40.0 kV, 30.0 mA). The total number of runs and images was based on the strategy calculation from the program **CrysAlisPro** (Rigaku, V1.171.39.9g, 2015). The maximum resolution achieved was Θ = 70.055°.

Cell parameters were retrieved using the **CrysAlisPro** (Rigaku, V1.171.39.9g, 2015) software and refined using **CrysAlisPro** (Rigaku, V1.171.39.9g, 2015) on 14528 reflections, 68 % of the observed reflections.

Data reduction was performed using the **CrysAlisPro** (Rigaku, V1.171.39.9g, 2015) software which corrects for Lorentz polarisation. The final completeness is 99.90 % out to 70.055° in Θ. The absorption coefficient μ of this material is 9.127 mm^{-1} at this wavelength (λ = 1.54184Å) and the minimum and maximum transmissions are 0.56461 and 1.00000..

The structure was solved in the space group C2/c (# 15) by Intrinsic Phasing using the **ShelXT** (Sheldrick, 2015) structure solution program and refined by Least Squares using version 2014/7 of **ShelXL** (Sheldrick, 2015). All non-hydrogen atoms were refined anisotropically. Hydrogen atom positions were calculated geometrically and refined using the riding model.

_exptl_absorpt_process_details: CrysAlisPro 1.171.39.9g (Rigaku Oxford Diffraction, 2015)Empirical absorption correction using spherical harmonics, implemented in SCALE3 ABSPACK scaling algorithm.

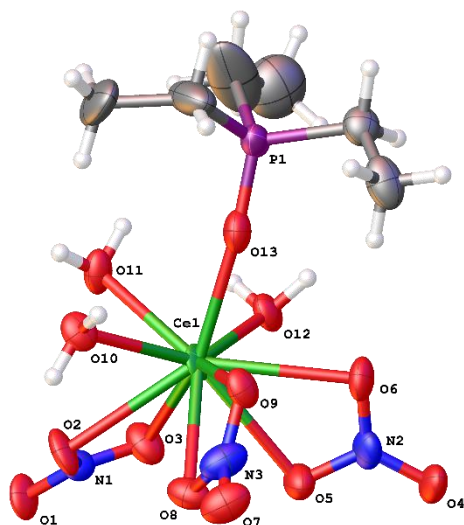# Crystal Data and Experimental for $Ce(NO_3)_3(H_2O)_3(Et_3PO)$

Figure 1: Thermal ellipsoids drawn at the 50% probability level.

Experimental. Single colourless plate-shaped crystals of **2017ncs0512** were obtained by recrystallisation from chloroform. A suitable crystal (0.050×0.030×0.005) mm³ was selected and mounted on a MITIGEN holder in perfluoroether oil on a Rigaku FRE+ diffractometer equipped with VHF Varimax confocal mirrors and an AFC12 goniometer and HyPix 6000 detector. The crystal was kept at T = 100(2) K during data collection. Using Olex2 (Dolomanov et al., 2009), the structure was solved the structure was solved with the ShelXT (Sheldrick, 2015) structure solution program, using the Intrinsic Phasing solution method. The model was refined with version 2014/7 of ShelXL (Sheldrick, 2015) using Least Squares minimisation.

Crystal Data. $C_6H_{21}N_3O_{13}PCe$, M_r = 514.35, orthorhombic, Aea2 (No. 41), a = 18.7948(9) Å, b = 13.9783(6) Å, c = 14.0130(5) Å, $\alpha = \beta = \gamma = 90°$, V = 3681.5(3) Å³, T = 100(2) K, Z = 8, Z' = 1, μ(MoK$_\alpha$) = 2.624 mm⁻¹, 40394 reflections measured, 4245 unique (R_{int} = 0.1121) which were used in all calculations. The final wR_2 was 0.2031 (all data) and R_1 was 0.0791 (I > 2(I)).

Compound	2017ncs0512
Formula	$C_6H_{21}N_3O_{13}PCe$
$D_{calc.}$/ g cm⁻³	1.856
μ/mm⁻¹	2.624
Formula Weight	514.35
Colour	colourless
Shape	plate
Size/mm³	0.050×0.030×0.005
T/K	100(2)
Crystal System	orthorhombic
Flack Parameter	0.007(16)
Hooft Parameter	0.033(11)
Space Group	Aea2
a/Å	18.7948(9)
b/Å	13.9783(6)
c/Å	14.0130(5)
α/°	90
β/°	90
γ/°	90
V/Å³	3681.5(3)
Z	8
Z'	1
Wavelength/Å	0.71075
Radiation type	MoK$_\alpha$
Θ_{min}/°	2.167
Θ_{max}/°	27.484
Measured Refl.	40394
Independent Refl.	4245
Reflections Used	4064
R_{int}	0.1121
Parameters	223
Restraints	1
Largest Peak	4.848
Deepest Hole	-2.853
GooF	1.115
wR_2 (all data)	0.2031
wR_2	0.2016
R_1 (all data)	0.0815
R_1	0.0791

Structure Quality Indicators

Reflections:

d min (Mo)	I/σ	Rint	complete at 2θ=55°
0.77	17.0	11.21%	100%

Refinement:

Shift	Max Peak	Min Peak	GooF	
0.000	4.8	-2.9	1.115	0.007(16)

A colourless plate-shaped crystal with dimensions 0.050×0.030×0.005 mm^3 was mounted on a MITIGEN holder in perfluoroether oil. X-ray diffraction data were collected using a Rigaku FRE+ diffractometer equipped with VHF Varimax confocal mirrors and an AFC12 goniometer and HyPix 6000 detector and equipped with an Oxford Cryosystems low-temperature device, operating at T = 100(2) K.

Data were measured using profile data from ω-scans of 0.5 ° per frame for 15.0 s using MoK$_\alpha$ radiation (Rotating Anode, 45.0 kV, 55.0 mA). The total number of runs and images was based on the strategy calculation from the program **CrysAlisPro** (Rigaku, V1.171.39.30d, 2017). The maximum resolution achieved was Θ = 27.484°.

Cell parameters were retrieved using the **CrysAlisPro** (Rigaku, V1.171.39.30d, 2017) software and refined using **CrysAlisPro** (Rigaku, V1.171.39.30d, 2017) on 9800 reflections, 24 % of the observed reflections.

Data reduction was performed using the **CrysAlisPro** (Rigaku, V1.171.39.30d, 2017) software which corrects for Lorentz polarisation. The final completeness is 100.00 % out to 27.484° in Θ.

A multi-scan absorption correction was performed using CrysAlisPro 1.171.39.30d (Rigaku Oxford Diffraction, 2017) Empirical absorption correction using spherical harmonics, implemented in SCALE3 ABSPACK scaling algorithm. The absorption coefficient μ of this material is 2.624 mm^{-1} at this wavelength (λ = 0.71075Å) and the minimum and maximum transmissions are 0.65235 and 1.00000.

The structure was solved in the space group Aea2 (# 41) by Intrinsic Phasing using the ShelXT (Sheldrick, 2015) structure solution program and refined by Least Squares using version 2014/7 of **ShelXL** (Sheldrick, 2015). All non-hydrogen atoms were refined anisotropically. Hydrogen atom positions were calculated geometrically and refined using the riding model.

There is a single molecule in the asymmetric unit, which is represented by the reported sum formula. In other words: Z is 8 and Z' is 1.

The Flack parameter was refined to 0.007(16). Determination of absolute structure using Bayesian statistics on Bijvoet differences using the Olex2 results in 0.033(11). Note: The Flack parameter is used to determine chirality of the crystal studied, the value should be near 0, a value of 1 means that the stereochemistry is wrong and the model should be inverted. A value of 0.5 means that the crystal consists of a racemic mixture of the two enantiomers.

Crystal Data and Experimental for [Ce(NO$_3$)$_3$(Et$_3$PO)$_3$][NO$_3$]
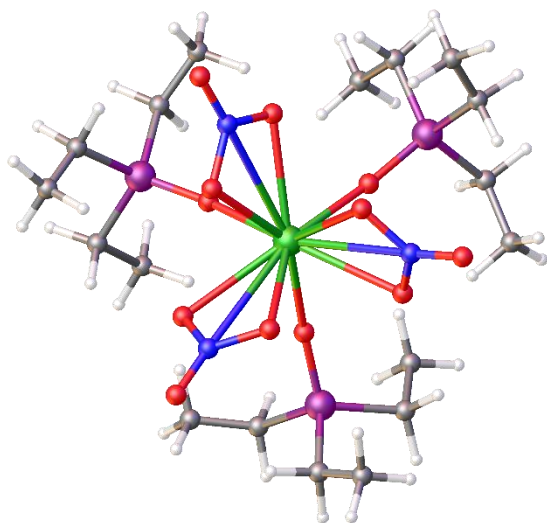

Figure 1: Thermal ellipsoids drawn at the 50% probability level

Experimental. A suitable light yellow block-shaped crystal of **2018ncs0267** (0.300×0.250×0.150 mm³) was selected and mounted on a MITIGEN holder in perfluoroether oil on a Rigaku FRE+ diffractometer equipped with VHF Varimax confocal mirrors and an AFC12 goniometer and HyPix 6000HE detector. The crystal was kept at a steady T = 100.00(10) K during data collection. The structure was solved with the **ShelXT** (Sheldrick, 2015) structure solution program using the Intrinsic Phasing solution method and by using **Olex2** (Dolomanov et al., 2009) as the graphical interface. The model was refined with version 2014/7 of **ShelXL** (Sheldrick, 2015) using Least Squares minimisation.

Crystal Data. C$_{18}$H$_{45}$CeN$_3$O$_{12}$P$_3$, M_r = 728.60, hexagonal, $P6_3$ (No. 173), a = 16.2791(3) Å, b = 16.2791(3) Å, c = 8.3776(2) Å, α = 90°, β = 90°, γ = 120°, V = 1922.69(9) Å³, T = 100.00(10) K, Z = 1.99998, Z' = 0.33333, μ(MoK$_\alpha$) = 1.354 mm⁻¹, 86383 reflections measured, 2941 unique (R_{int} = 0.0639) which were used in all calculations. The final wR_2 was 0.1338 (all data) and R_1 was 0.0503 (I > 2(I)).

Compound	2018ncs0267
Formula	C$_{18}$H$_{45}$CeN$_3$O$_{12}$P$_3$
$D_{calc.}$/ g cm⁻³	1.259
μ/mm⁻¹	1.354
Formula Weight	728.60
Colour	light yellow
Shape	block
Size/mm³	0.300×0.250×0.150
T/K	100.00(10)
Crystal System	hexagonal
Flack Parameter	0.300(11)
Hooft Parameter	0.266(4)
Space Group	$P6_3$
a/Å	16.2791(3)
b/Å	16.2791(3)
c/Å	8.3776(2)
α/°	90
β/°	90
γ/°	120
V/Å³	1922.69(9)
Z	1.99998
Z'	0.33333
Wavelength/Å	0.71075
Radiation type	MoK$_\alpha$
Θ_{min}/°	2.502
Θ_{max}/°	27.484
Measured Refl.	86383
Independent Refl.	2941
Reflections with I > 2(I)	2839
R_{int}	0.0639
Parameters	106
Restraints	1
Largest Peak	1.980
Deepest Hole	-0.430
GooF	1.071
wR_2 (all data)	0.1338
wR_2	0.1324
R_1 (all data)	0.0518
R_1	0.0503

Structure Quality Indicators

Reflections:

d min (Mo)	I/σ	Rint	complete 100% (IUCr)
0.77	73.7	6.39%	100%

Refinement:

Shift	Max Peak	Min Peak	GooF	Flack
0.000	2.0	-0.4	1.071	.300(11)

A light yellow block-shaped crystal with dimensions 0.300×0.250×0.150 mm³ was mounted on a MITIGEN holder in perfluoroether oil. Data were collected using a Rigaku FRE+ diffractometer equipped with VHF Varimax confocal mirrors and an AFC12 goniometer and HyPix 6000HE detector, and equipped with an Oxford Cryosystems low-temperature device operating at T = 100.00(10) K.

Data were measured using ω scans of 0.5 ° per frame for 1 s using MoK$_\alpha$ radiation. The total number of runs and images was based on the strategy calculation from the program **CrysAlisPro** (Rigaku, V1.171.39.46, 2018). The maximum resolution that was achieved was Θ = 27.484° (0.77 Å).

Cell parameters were retrieved using the **CrysAlisPro** (Rigaku, V1.171.39.46, 2018) software and refined using **CrysAlisPro** (Rigaku, V1.171.39.46, 2018) on 27221 reflections, 32% of the observed reflections.

Data reduction, scaling and absorption corrections were performed using **CrysAlisPro** (Rigaku, V1.171.39.46, 2018). The final completeness is 99.90 % out to 27.484° in Θ.

A multi-scan absorption correction was performed using CrysAlisPro 1.171.39.46 (Rigaku Oxford Diffraction, 2018) using spherical harmonics as implemented in SCALE3 ABSPACK. The absorption coefficient μ of this material is 1.354 mm⁻¹ at this wavelength (λ = 0.711Å) and the minimum and maximum transmissions are 0.530 and 1.000.

The structure was solved and the space group $P6_3$ (# 173) determined by the **ShelXT** (Sheldrick, 2015) structure solution program using Intrinsic Phasing and refined by Least Squares using version 2014/7 of **ShelXL** (Sheldrick, 2015). All non-hydrogen and non-carbon atoms were refined anisotropically. The disordered carbon atoms were refined isotropically, together with the occupancy factors for part 1 and part 2. Hydrogen atom positions were calculated geometrically and refined using the riding model. The CH3 hydrogens were geometrically calculated (AFIX 33). There are voids (channels) in the structure of about 360 Å³. No obvious solvent molecules were found, so the structure was SQUEEZEd.

The value of Z' is 0.33333.

The Flack parameter was refined to 0.300(11). Determination of absolute structure using Bayesian statistics on Bijvoet differences using the Olex2 results in 0.266(4). Note: The Flack parameter is used to determine chirality of the crystal studied, the value should be near 0, a value of 1 means that the stereochemistry is wrong and the model should be inverted. A value of 0.5 means that the crystal consists of a racemic mixture of the two enantiomers.

The crystal has disordered Et groups, part 1 and part 2. The occupancy of the groups was refined as 0.53(1) and 0.47(1) respectively, so not significantly different from 0.5-0.5.

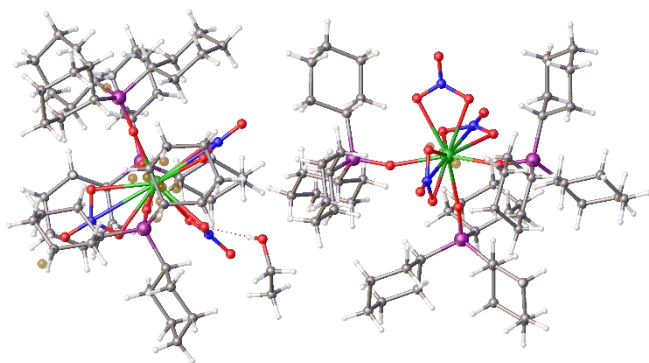# Crystal Data and Experimental for $Ce(NO_3)_3(Cy_3PO)_3$

Figure 1: Thermal ellipsoids drawn at the 50% probability level.

Experimental. A suitable colourless block-shaped crystal of **2018ncs0521** (0.400×0.300×0.100 mm^3) was selected and mounted on a MITIGEN holder in perfluoroether oil on an Rigaku FRE+ diffractometer equipped with VHF Varimax confocal mirrors and an AFC12 goniometer and HyPix 6000HE detector. The crystal was kept at a steady T = 100.00(10) K during data collection. The structure was solved with the **ShelXT** (Sheldrick, 2015) structure solution program using the Intrinsic Phasing solution method and by using **Olex2** (Dolomanov et al., 2009) as the graphical interface. The model was refined with version 2014/7 of **ShelXL** (Sheldrick, 2015) using Least Squares minimisation.

Crystal Data. $C_{110}H_{204}Ce_2N_6O_{25}P_6$, M_r = 2476.84, monoclinic, $P2_1$ (No. 4), a = 11.71280(10) Å, b = 18.73370(10) Å, c = 28.5137(2) Å, β = 100.1860(10)°, α = γ = 90°, V = 6157.98(8) Å^3, T = 100(2) K, Z = 2, Z' = 1, μ(MoK$_\alpha$) = 0.876 mm^{-1}, 282488 reflections measured, 28239 unique (R_{int} = 0.0667) which were used in all calculations. The final wR_2 was 0.0777 (all data) and R_1 was 0.0306 (I > 2(I)).

Compound	2018ncs0521
Formula	$C_{110}H_{204}Ce_2N_6O_{25}P_6$
$D_{calc.}$/ g cm^{-3}	1.336
μ/mm^{-1}	0.876
Formula Weight	2476.84
Colour	colourless
Shape	block
Size/mm^3	0.400×0.300×0.100
T/K	100.00(10)
Crystal System	monoclinic
Flack Parameter	-0.018(5)
Hooft Parameter	-0.0020(16)
Space Group	$P2_1$
a/Å	11.71280(10)
b/Å	18.73370(10)
c/Å	28.5137(2)
α/°	90
β/°	100.1860(10)
γ/°	90
V/Å^3	6157.98(8)
Z	2
Z'	1
Wavelength/Å	0.71075
Radiation type	MoK$_\alpha$
Θ_{min}/°	1.767
Θ_{max}/°	27.485
Measured Refl.	282488
Independent Refl.	28239
Reflections with I > 2(I)	27612
R_{int}	0.0667
Parameters	1344
Restraints	1
Largest Peak	1.079
Deepest Hole	-0.962
GooF	1.051
wR_2 (all data)	0.0777
wR_2	0.0773
R_1 (all data)	0.0314
R_1	0.0306

Structure Quality Indicators

Reflections:

d min (Mo)	I/σ	Rint	complete 100% (IUCr)
0.77	35.5	6.67%	100%

Refinement:

Shift	Max Peak	Min Peak	GooF	Flack
-0.001	1.1	-1.0	1.051	-.018(5)

A colourless block-shaped crystal with dimensions 0.400×0.300×0.100 mm³ was mounted on a MITIGEN holder in perfluoroether oil. Data were collected using a Rigaku FRE+ diffractometer equipped with VHF Varimax confocal mirrors and an AFC12 goniometer and HyPix 6000HE detectore, and quipped with an Oxford Cryosystems low-temperature device operating at T = 100.00(10) K.

Data were measured using ω scans of 0.5 ° per frame for 0.5 s using MoK$_\alpha$ radiation (Rotating-anode X-ray tube, 40 kV, 30 mA). The total number of runs and images was based on the strategy calculation from the program **CrysAlisPro** (Rigaku, V1.171.39.46, 2018). The maximum resolution that was achieved was Θ = 27.485° (0.77 Å).

Cell parameters were retrieved using the **CrysAlisPro** (Rigaku, V1.171.39.46, 2018) software and refined using **CrysAlisPro** (Rigaku, V1.171.39.46, 2018) on 192437 reflections, 68% of the observed reflections.

Data reduction, scaling and absorption corrections were performed using **CrysAlisPro** (Rigaku, V1.171.39.46, 2018). The final completeness is 100.00 % out to 27.485° in Θ.

A multi-scan absorption correction was performed using CrysAlisPro 1.171.39.46 (Rigaku Oxford Diffraction, 2018) using spherical harmonics as implemented in SCALE3 ABSPACK. The absorption coefficient μ of this material is 0.876 mm⁻¹ at this wavelength (λ = 0.71075Å) and the minimum and maximum transmissions are 0.402 and 1.000.

The structure was solved and the space group $P2_1$ (# 4) determined by the **ShelXT** (Sheldrick, 2015) structure solution program using Intrinsic Phasing and refined by Least Squares using version 2014/7 of **ShelXL** (Sheldrick, 2015). All non-hydrogen atoms were refined anisotropically. Hydrogen atom positions were calculated geometrically and refined using the riding model.

There is a single molecule in the asymmetric unit, which is represented by the reported sum formula. In other words: Z is 2 and Z' is 1. However, there are actually 2 Ce molecules and 1 ethanol per asymmetric unit.

The Flack parameter was refined to -0.018(5). Determination of absolute structure using Bayesian statistics on Bijvoet differences using the Olex2 results in -0.0020(16). Note: The Flack parameter is used to determine chirality of the crystal studied, the value should be near 0, a value of 1 means that the stereochemistry is wrong and the model should be inverted. A value of 0.5 means that the crystal consists of a racemic mixture of the two enantiomers.

Table S2 13-C data for Ce(NO$_3$)$_4$(R$_3$PO)$_2$ in CDCl$_3$

Ce(NO$_3$)$_4$(R$_3$PO)$_2$	CH$_3$	CH$_2$	CH	C
Et$_3$PO	4.95(d) $^2J_{PC}$ 5 Hz	18.35 $^1J_{PC}$ 65 Hz		
^{i}Pr	17.85 (s)		27.31(d) $^1J_{PC}$ 61 Hz	
^{n}Bu	13.48 (s)	25.8 (d) $^1J_{PC}$ 63 Hz 24.0 (d) $^2J_{PC}$ 15 Hz 23.0 (s)		
^{i}Bu	24.04(d) $^2J_{PC}$ 9 Hz	36.31 (d) $^1J_{PC}$ 61 Hz	23.04 (d) $^2J_{PC}$ 8 Hz	
^{t}Bu	28.97(s)			39.31(d) $^1J_{PC}$ 63 Hz
Cy		26.78(d) $^2J_{PC}$ 12 Hz 25.64 (d) $^3J_{PC}$ 3 Hz 25.73 (s)	35.39 (d) $^1J_{PC}$ 58 Hz	
Oct	14.18(s)	26.07 (d) $^1J_{PC}$ 63 Hz 31.09 (d) $^2J_{PC}$ 17 Hz 21.02 (d) $^3J_{PC}$ 3 Hz 31.8 (s) 29.04 (s) 28.93 (s)		

Table S2 Selected bond lengths

$Ce(NO_3)_4(Cy_3PO)_2$
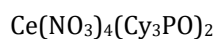
Atom	Atom	Length/Å
Ce1	O1[1]	2.239(3)
Ce1	O1	2.240(3)
Ce1	O3[1]	2.478(3)
Ce1	O3	2.478(3)
Ce1	O4[1]	2.506(4)
Ce1	O4	2.506(4)
Ce1	O6[1]	2.472(3)
Ce1	O6	2.472(3)
Ce1	O7[1]	2.476(3)

$[Ce(NO_3)_3(Cy_3PO)_3]$
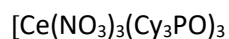
Atom	Atom	Length/Å
Ce1	O1	2.368(3)
Ce1	O2	2.400(2)
Ce1	O3	2.382(2)
Ce1	O4	2.597(3)
Ce1	O6	2.603(3)
Ce1	O7	2.565(3)
Ce1	O9	2.603(3)
Ce1	O10	2.634(3)
Ce1	O12	2.619(3)

$Ce(NO_3)_3(H_2O)_3(Et_3PO)$
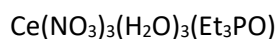
Atom	Atom	Length/Å
Ce1	O2	2.656(13)
Ce1	O3	2.693(15)
Ce1	O5	2.625(15)
Ce1	O6	2.653(14)
Ce1	O8	2.614(14)
Ce1	O9	2.670(13)
Ce1	O10	2.515(15)
Ce1	O11	2.501(14)
Ce1	O12	2.519(15)
Ce1	O13	2.318(16)

$[Ce(NO_3)_3(Et_3PO)_3][NO_3]CHCl_3.$

Atom	Atom	Length/Å
Ce1	O1[2]	2.455(7)
Ce1	O1[3]	2.455(7)
Ce1	O1	2.455(7)
Ce1	O2[3]	2.509(6)
Ce1	O2[2]	2.509(6)
Ce1	O2	2.509(6)
Ce1	O4[2]	2.199(7)
Ce1	O4	2.199(7)
Ce1	O4[3]	2.199(7)

[1]1-x,+y,1/2-z   [2]1+y-x,1-x,+z; [3]1-y,+x-y,+z